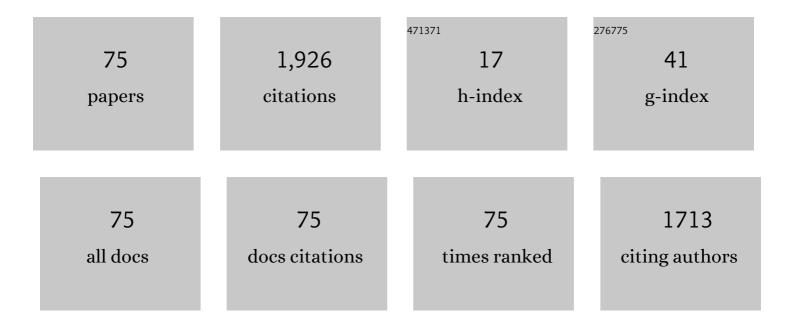
List of Publications by Year in descending order

Source: https://exaly.com/author-pdf/1466441/publications.pdf Version: 2024-02-01



KENNETH DVMOND

#	Article	IF	CITATIONS
1	RENU2 UV PMT Observations of the Cusp. Geophysical Research Letters, 2020, 47, e2019GL082314.	1.5	2
2	Initial Observations by the GOLD Mission. Journal of Geophysical Research: Space Physics, 2020, 125, e2020JA027823.	0.8	80
3	A Comparison of Electron Densities Derived by Tomographic Inversion of the 135.6â€nm Ionospheric Nightglow Emission to Incoherent Scatter Radar Measurements. Journal of Geophysical Research: Space Physics, 2019, 124, 4585-4596.	0.8	7
4	Coordinated Ionospheric Reconstruction CubeSat Experiment (CIRCE) mission overview. , 2019, , .		6
5	Comparison of second and third generation 135.6 nm ionospheric photometers using on-orbit and laboratory results. , 2019, , .		3
6	Ultraviolet beam splitter characterization for use in a CubeSat optical system. Journal of Applied Remote Sensing, 2019, 13, 1.	0.6	4
7	Evaluating Different Techniques for Constraining Lower Atmospheric Variability in an Upper Atmosphere General Circulation Model: A Case Study During the 2010 Sudden Stratospheric Warming. Journal of Advances in Modeling Earth Systems, 2018, 10, 3076-3102.	1.3	11
8	Evaluation of UV optics for Triple Tiny Ionospheric Photometers on CubeSat missions. , 2018, , .		3
9	The Special Sensor Ultraviolet Limb Imager instruments. Journal of Geophysical Research: Space Physics, 2017, 122, 2674-2685.	0.8	9
10	lonosphericâ€thermospheric UV tomography: 1. Image space reconstruction algorithms. Radio Science, 2017, 52, 338-356.	0.8	12
11	Evaluation of the performance of ionospheric models at solar maximum using COSMIC slant TEC measurements. Radio Science, 2017, 52, 378-388.	0.8	2
12	Ionosphericâ€ŧhermospheric UV tomography: 3. A multisensor technique for creating fullâ€orbit reconstructions of atmospheric UV emission. Radio Science, 2017, 52, 896-916.	0.8	3
13	The Global-Scale Observations of the Limb and Disk (GOLD) Mission. Space Science Reviews, 2017, 212, 383-408.	3.7	105
14	lonosphericâ€ŧhermospheric UV tomography: 2. Comparison with incoherent scatter radar measurements. Radio Science, 2017, 52, 357-366.	0.8	8
15	Low-latitude ionospheric research using the CIRCE Mission: instrumentation overview. , 2017, , .		3
16	The Tiny Ionospheric Photometer (TIP) on the Constellation Observing System for Meteorology, Ionosphere, and Climate (COSMIC/FORMOSAT-3). Journal of Geophysical Research: Space Physics, 2016, 121, 10,614-10,622.	0.8	8
17	Stellar calibration of the Special Sensor Ultraviolet Limb Imager (SSULI) on the DMSP spacecraft. Proceedings of SPIE, 2015, , .	0.8	3
18	Simulations of the effects of vertical transport on the thermosphere and ionosphere using two coupled models. Journal of Geophysical Research: Space Physics, 2014, 119, 1172-1185.	0.8	39

#	Article	IF	CITATIONS
19	New Systems for Space Based Monitoring of Ionospheric Irregularities and Radio Wave Scintillations. Geophysical Monograph Series, 2013, , 431-440.	0.1	7
20	A new technique for spectral analysis of ionospheric TEC fluctuations observed with the Very Large Array VHF system: From QP echoes to MSTIDs. Radio Science, 2012, 47, .	0.8	24
21	Highâ€precision measurements of ionospheric TEC gradients with the Very Large Array VHF system. Radio Science, 2012, 47, .	0.8	23
22	Global observations of L band scintillation at solar minimum made by COSMIC. Radio Science, 2012, 47, .	0.8	37
23	A mediumâ€scale traveling ionospheric disturbance observed from the ground and from space. Radio Science, 2011, 46, .	0.8	14
24	A study of the strong linear relationship between the equatorial ionization anomaly and the prereversal E × B drift velocity at solar minimum. Radio Science, 2011, 46, .	0.8	14
25	Horizontal Ionospheric Electron Density Gradients Observed by FORMOSAT-3/COSMIC TIP: Spatial Distributions and Effects on VLF Wave Propagation at Mid-Latitudes. Terrestrial, Atmospheric and Oceanic Sciences, 2009, 20, 251.	0.3	2
26	Tomographic Reconstruction of the Low-Latitude Nighttime Electron Density Using FORMOSAT-3/COMSIC Radio Occultation and UV Photometer Data. Terrestrial, Atmospheric and Oceanic Sciences, 2009, 20, 215.	0.3	10
27	Ionospheric Electron Density Concurrently Derived by TIP and GOX of FORMOSAT-3/COSMIC. Terrestrial, Atmospheric and Oceanic Sciences, 2009, 20, 207.	0.3	7
28	Observations of the Ionosphere Using the Tiny Ionospheric Photometer. Terrestrial, Atmospheric and Oceanic Sciences, 2009, 20, 227.	0.3	12
29	Simultaneous radio interferometer and optical observations of ionospheric structure at the Very Large Array. Radio Science, 2009, 44, .	0.8	11
30	Remote sensing of nighttime <i>F</i> region peak height and peak density using ultraviolet line ratios. Radio Science, 2009, 44, .	0.8	8
31	Tiny Ionospheric Photometers on FORMOSAT-3/COSMIC: on-orbit performance. , 2009, , .		8
32	On-orbit calibration of the Tiny Ionospheric Photometer on the COSMIC/FORMOSAT-3 satellites. , 2009,		6
33	Hemispheric asymmetries in the longitudinal structure of the lowâ€latitude nighttime ionosphere. Journal of Geophysical Research, 2008, 113, .	3.3	25
34	The COSMIC/FORMOSAT-3 Mission: Early Results. Bulletin of the American Meteorological Society, 2008, 89, 313-334.	1.7	783
35	Application of SSULI ground calibration methods to retrieval of spectral emissions on flight instruments. Proceedings of SPIE, 2007, , .	0.8	1
36	Observations of middle ultraviolet emissions in the middle and lower thermosphere: NO, O ₂ , O, and Mg ⁺ . Journal of Geophysical Research, 2007, 112, .	3.3	5

#	Article	IF	CITATIONS
37	Validation of nighttime UV measurements of theFregion ionosphere made by the low resolution airglow and aurora spectrograph (LORAAS) instrument. Radio Science, 2006, 41, n/a-n/a.	0.8	1
38	Simultaneous inversion of total electron content and UV radiance data to produceFregion electron densities. Radio Science, 2006, 41, n/a-n/a.	0.8	1
39	Preparing for COSMIC: Inversion and Analysis of Ionospheric Data Products. , 2006, , 137-146.		40
40	The optomechanical design and operation of the ionospheric mapping and geocoronal experiment. , 2005, , .		3
41	Ionospheric response to the solar flare of 14 July 2000. Radio Science, 2004, 39, n/a-n/a.	0.8	13
42	Middle and upper thermospheric odd nitrogen: 2. Measurements of nitric oxide from Ionospheric Spectroscopy and Atmospheric Chemistry (ISAAC) satellite observations of NO γ band emission. Journal of Geophysical Research, 2004, 109, .	3.3	14
43	Comparison of ionospheric observations from UV limb scans and radar altimetry. Radio Science, 2004, 39, n/a-n/a.	0.8	2
44	Oxygen aurora during the recovery phase of a major geomagnetic storm. Journal of Geophysical Research, 2004, 109, .	3.3	6
45	The tiny ionospheric photometer instrument design and operation. , 2004, 5660, 259.		5
46	Middle ultraviolet emission from ionized iron. Geophysical Research Letters, 2003, 30, 3-1-3-4.	1.5	67
47	Quenching rate coefficients for O+(2P) derived from middle ultraviolet airglow. Journal of Geophysical Research, 2003, 108, .	3.3	22
48	<title>Volumetric imaging system for the ionosphere (VISION)</title> ., 2002, , .		0
49	<title>On-orbit characterization and performance of the HIRAAS instruments aboard ARGOS: LORAAS sensor performance</title> . , 2002, , .		5
50	<title>Experiment for studying spatial and temporal behavior of the ionosphere</title> . , 2002, 4485, 266.		2
51	Comparison of O+density from ARGOS LORAAS data analysis and SAMI2 model results. Geophysical Research Letters, 2002, 29, 6-1.	1.5	22
52	lonospheric and dayglow responses to the radiative phase of the Bastille Day flare. Geophysical Research Letters, 2002, 29, 99-1-99-4.	1.5	50
53	Electron densities determined by the HIRAAS Experiment and comparisons with ionosonde measurements. Geophysical Research Letters, 2001, 28, 927-930.	1.5	14
54	An algorithm for inferring the two-dimensional structure of the nighttime ionosphere from radiative recombination measurements. Radio Science, 2001, 36, 1241-1254.	0.8	14

#	Article	IF	CITATIONS
55	A technique for using measured ionospheric density gradients and GPS occultations for inferring the nighttime ionospheric electron density. Radio Science, 2001, 36, 1141-1148.	0.8	10
56	Electron densities determined by inversion of ultraviolet limb profiles. Journal of Geophysical Research, 2001, 106, 30315-30321.	3.3	12
57	O+, O, and O2densities derived from measurements made by the High Resolution Airglow/Aurora Spectrograph (HIRAAS) sounding rocket experiment. Journal of Geophysical Research, 2000, 105, 23025-23033.	3.3	11
58	The Tiny Ionospheric Photometer: An Instrument for Measuring Ionospheric Gradients for the COSMIC Constellation. Terrestrial, Atmospheric and Oceanic Sciences, 2000, 11, 273.	0.3	15
59	<title>Update on the calibration and performance of the special sensor ultraviolet limb imagers
(SSULI)</title> . , 1999, 3818, 90.		9
60	<title>High-resolution Ionospheric and Thermospheric Spectrograph (HITS) on the Advanced Research
and Global Observing Satellite (ARGOS): quick look results</title> . , 1999, , .		7
61	<title>Spectral fitting applications: improved calibration and radiometric accuracy of EUV/FUV sensors</title> . , 1999, , .		2
62	<title>Ionospheric Spectroscopy and Atmospheric Chemistry (ISAAC) experiment on the Advanced
Research and Global Observation Satellite (ARGOS): quick look results</title> . , 1999, , .		11
63	<title>High-Resolution Airglow and Aurora Spectrograph (HIRAAS) sounding rocket
experiment</title> ., 1999, 3818, 126.		2
64	Atomic and molecular emissions in the middle ultraviolet dayglow. Journal of Geophysical Research, 1998, 103, 29215-29228.	3.3	11
65	Two-dimensional mapping of the plasma density in the upper atmosphere with computerized ionospheric tomography (CIT). Physics of Plasmas, 1998, 5, 2010-2021.	0.7	54
66	Discrete inverse theory for 834-Ã ionospheric remote sensing. Radio Science, 1997, 32, 1973-1984.	0.8	19
67	An optical remote sensing technique for determining nighttimeFregion electron density. Radio Science, 1997, 32, 1985-1996.	0.8	53
68	Investigation of ionospheric O+remote sensing using the 834-Ã airglow. Journal of Geophysical Research, 1997, 102, 2441-2456.	3.3	27
69	Effect of energetic electron and proton bombardment on the reflectance of silicon-carbide mirrors in the extreme-ultraviolet region. Applied Optics, 1994, 33, 5902.	2.1	3
70	Effect of oxygen atom bombardment on the reflectance of silicon carbide mirrors in the extreme ultraviolet region. Applied Optics, 1993, 32, 1805.	2.1	9
71	<title>Ultraviolet spectrographs for thermospheric and ionospheric remote sensing</title> . , 1993, 1940, 117.		8
72	<title>Effect of oxygen atom bombardment on the reflectance of SiC mirrors in the</td><td></td><td>2</td></tr></tbody></table></title>		

extreme-ultraviolet region </title>., 1993, , .

#	Article	IF	CITATIONS
73	<title>A far and extreme ultraviolet limb imaging spectrograph for DMSP satellites</title> . , 1992, , .		17
74	The atomic carbon distribution in the coma of comet P/Halley. , 1988, , 380-384.		1
75	Rocket ultraviolet spectroscopy of comet Halley and abundance of carbon monoxide and carbon. Nature, 1986, 324, 436-438.	13.7	57